Cellular Physiology and Biochemistry

Cell Physiol Biochem 2018;51:2290-2308
DOI: 10.1159/000495873
Published online: 7 December 2018
Accepted: 29 November 2018

© 2018 The Author(s)
Published by S. Karger AG, Basel
www.karger.com/cpb

Karger Open access

This article is licensed under the Creative Commons Attribution-NonCommercial-NoDerivatives 4.0 International License (CC BY-NC-ND) (http://www.karger.com/Services/OpenAccessLicense). Usage and distribution for commercial purposes as well as any distribution of modified material requires written permission.

Original Paper

Dental Follicle Stem Cells Ameliorate Lipopolysaccharide-Induced Inflammation by Secreting TGF-β3 and TSP-1 to Elicit Macrophage M2 Polarization

Xiaochuan Chen[a,b] Bo Yang[a,b] Jun Tian[a,b] Hong Hong[a,b] Yu Du[a,b] Kun Li[c] Xin Li[a,b] Nan Wang[c] Xiaoqi Yu[c] Xi Wei[a,b]

[a]Guanghua School of Stomatology, Hospital of Stomatology, Sun Yat-sen University, Guangzhou, [b]Guangdong Provincial Key Laboratory of Stomatology, Guangzhou, [c]Key Laboratory of Green Chemistry and Technology, Ministry of Education, College of Chemistry, Sichuan University, Chengdu, China

Key Words
Dental follicle stem cells • Macrophages • Conditioned medium • Cytokines • Polarization • Acute lung injury

Abstract
Background/Aims: Increasing evidence has demonstrated the novel roles of mesenchymal stem cells (MSCs) in immunotherapy. However, difficulty in acquiring these cells and possible ethical issues limited their application. Recently, we have isolated a unique MSC population from dental follicles with potent stem cell-like properties. This study focused on the effects of dental follicle stem cells (DFSCs) on macrophage activation and polarization to determine their role in immunomodulation and to test if DFSCs are a promising cell source for MSC-based immunotherapy. ***Methods:*** Rat acute lung injury (ALI) models induced by Lipopolysaccharide (LPS) were applied to test the immune-modulatory effects of DFSC/DFSC-CM *in vivo*. The pulmonary permeability was determined by the dry / wet weight ratios of the left upper lung lobe. The lung histopathological damage was graded on a 0 to 4+ scale. And the inflammatory cytokines in bronchoalveolar lavage fluid (BALF) were tested by ELISA. Then we established LPS-induced inflamed macrophage models *in vitro*. Inflammatory cytokine production and polarization marker expression were measured by RT-qPCR, ELISA, western blot and flow cytometric analysis in macrophages following DFSC-CM treatment. The paracrine factors in DFSC-CM were revealed by a RayBiotech Protein Array. Thereafter, neutralization studies were performed to confirm the potential immune regulators in DFSC-CM. ***Results:*** The DFSC/DFSC-CM not only attenuated histopathological damage and pulmonary permeability, but also downregulated pro-inflammatory cytokines MCP-1, IL-1, IL-6 and TNF-α, and upregulated anti-inflammatory cytokine IL-10 in BALF. Immunofluorescence staining revealed

X. Chen and B. Yang contributed equally to this work.

Dr. Xi Wei
and Prof. Xiaoqi Yu
Dept. of Operative Dent. and Endodontics, Guanghua School of Stomatology, Sun Yat-sen Univ.;
Key Lab. of Green Chem. and Tech., Min. of Education, College of Chem., Sichuan Univ., Guangzhou (China)
Tel. (86-20) 83880049, Fax (86-20) 83822807, E-Mail weixi@mail.sysu.edu.cn; xqyu@scu.edu.cn

the increased expression of macrophage M2 marker Arg-1. Further *in vitro* study revealed that macrophages switched to an anti-inflammatory M2 phenotype when co-cultured with DFSC-CM, characterized by suppressed production of pro-inflammatory cytokines MCP-1, IL-1, IL-6, TNF-α and M1-polarizing markers iNOS and CD86; and increased expression of the anti-inflammatory cytokine IL-10 and the M2-polarizing markers Arg-1 and CD163. A RayBiotech Protein Array revealed 42 differentially expressed (>2-fold) paracrine factors in DFSC-CM compared with the serum-free Ham's F-12K medium, among which TGF-β3 and Thrombospondin-1 (TSP-1) were upregulated by 18- and 105-fold, respectively. Neutralization studies confirmed the immunoregulatory roles of TGF-β3 and TSP-1 in macrophage activation and polarization. ***Conclusion:*** These results indicated that DFSCs can reprogram macrophages into the anti-inflammatory M2 phenotype, the paracrine factors TGF-β3 and TSP-1 may be one of the underlying mechanisms. This study supports the hypothesis that DFSCs are promising for MSC-based immunotherapy.

© 2018 The Author(s)
Published by S. Karger AG, Basel

Introduction

Macrophages consist in basically all tissues. They are cellular components of the innate immune systems, ingesting and degrading dead cells, debris, and foreign material and orchestrating inflammatory processes [1-3]. They play a crucial role in tissue homeostasis, key immunological processes and the development of various diseases [4, 5]. Activated macrophages are critical for the clearance of invading pathogens and their toxic products and classified into M1 and M2 types [6]. M1 macrophages, which produce high levels of pro-inflammatory cytokines, nitric oxide (NO), and reactive oxygen species [7], are implicated in initiating and sustaining inflammation. However, the M2 subtype generates high levels of anti-inflammatory cytokines such as IL-10, TGF-β1 and PDGF[8] and facilitates anti-inflammatory activity [1]. The balance between M1 and M2 macrophages is essential for homeostasis, and a shift from M1-rich to M2-rich macrophages alleviates inflammatory processes and promotes tissue repair and regeneration [9, 10]. Therefore, inducing M1 to M2 switch in macrophages may be of vital importance and have promising applications in immunotherapy.

MSCs represent a heterogeneous population of spindle-shaped stromal cells, with self-renewal and colony-forming properties and multipotent differentiation capacities [11]. MSCs possess the unique ability of homing to inflammatory sites guided by various growth factors and cytokines so that the tissue may be repaired [12, 13]. Recently, MSCs have been shown to regulate immune responses by suppressing the proliferation and activation of T and B cells, and promote the generation of regulatory T cells, manifesting the immunosuppressive functions [13, 14]. In addition, MSCs elicit a phenotypic switch from M1 to M2 macrophages *in vitro* [15, 16] as well as in animal models of acute kidney injury [17], experimental colitis [18], spinal cord injury [19], and skin wounds [1]. MSCs affect neighboring immune cells primarily through direct cell–to-cell contact and/or various soluble factors [12-14, 20]. These novel properties indicate that MSCs are promising candidates in cell-based therapies for a variety of immune and inflammation-related diseases [12-14]. There are several clinical trials of MSCs for the treatment of immune and inflammation-related diseases, such as lupus erythematosus (NCT03171194), primary immunodeficiency diseases (NCT02579967), inflammatory bowel disease (NCT01851343), osteoarthritis (NCT02666443), ischemic disease (NCT03225625) and so on. Bone marrow is currently the most common source of MSCs [21]. However, difficulty in acquiring these cells and possible ethical issues limited their application. Therefore, there is an urgent need to find alternatives with easy access and reduced damage.

Recently, oral cavity have been paid more and more attention to gaining somatic stem cells as it's more flexible for the surgeons to harvest the tissues without undue trauma to the patients [22, 23]. Among them, the odontogenic stem cells are derived from extracted teeth in dentistry such as deciduous, orthodontic and wisdom teeth. They are much easier

to harvest and do not cause any secondary harm to individuals. Therefore, less ethical issues are involved. There are many kinds of odontogenic stem cells, such as dental pulp stem cells (DPSCs), dental follicle stem cells (DFSCs), stem cells from human exfoliated deciduous teeth (SHEDs) and so on. A growing number of studies have shown the immunomodulatory capacities of oral-derived stem cells, especially DPSCs and SHEDs. For instance, researchers applied SHED-conditioned medium to treat experimental autoimmune encephalomyelitis [24], rheumatoid arthritis [25] and systemic lupus erythematosus [26, 27]. The results showed that SHEDs had significantly reduced the tissue damage caused by autoimmune diseases. Possible mechanisms are the transplantation of SHEDs directly regulate the proportion of Th17 cells in T cells; on the other hand, the SHEDs paracrine factors directly inhibit inflammatory responses or indirectly facilitate M2 macrophages to exert inflammatory regulation. However, DFSCs exhibited an enhanced differentiation ability and could induce increased number of $CD4^+FoxP3^+$ Treg cells and suppressed the proliferation of peripheral blood mononuclear cells compared with DPSCs and SHEDs [28], suggesting that DFSCs might also have potent immune-regulation capability or even better. However, the effect of DFSCs on macrophage polarization remains unknown, which may be an important consideration in determining whether DFSCs can be used as novel alternative cells for MSC-based immunotherapy.

Recently, many studies reported that acute lung injury (ALI) animal model induced by Lipopolysaccharide (LPS)[29, 30], which is a progressive clinical disease with high mortality and characterized by an excessive and uncontrolled inflammatory response, could be applied to test the immune-modulatory effects *in vivo*. The theory is that in the development of ALI, neutrophils and macrophages are activated to eliminate pathogens, however, it brings tissue damage by releasing antimicrobial compounds at the same time [31]. And the treatment like MSCs or cytokines may make a change in the whole process, such as promoting macrophage M2 polarization [32].

In our previous study, we successfully isolated DFSCs from dental follicles and demonstrated that they highly expressed the reprogramming markers Oct-4, Sox-2 and MYC[33]. We also studied the modulation and differentiation of DFSCs [34-37]. In order to learn comprehensively the immune modulating properties of DFSCs, here we investigated the immunomodulatory effects of DFSCs on macrophage activation and polarization under inflammatory conditions in LPS-induced rat ALI models, as well as in a rat macrophage cell line. Furthermore, we explored the possible immunomodulatory paracrine factors to clarify the potential mechanisms of DFSC-directed macrophage polarization switch.

Materials and Methods

Isolation and culture of DFSCs

DFSCs were isolated and cultured as previously described [38]. Briefly, dental follicle tissues were harvested from 7-day-old Sprague-Dawley (S-D) rats, which were purchased from the Laboratory Animal Center of Sun Yat-sen University. Isolated dental follicle tissues were washed and finely minced into 1 mm small pieces and then incubated in 3 mg/ml collagenase I (Sigma-Aldrich, USA) and 4 mg/ml Dispase II (Sigma-Aldrich, USA) for 30 min at 37°C. Explants were then transferred to T25 cell culture flasks and cultivated in α minimum essential medium (α-MEM, Gibco, USA), supplemented with 20% fetal bovine serum (FBS, Gibco, USA), 100 U/ml penicillin (Gibco, USA) and 100 mg/ml streptomycin (Gibco, USA) at 37°C in a 5% CO_2 humidified atmosphere. The medium was changed every three days. The DFSCs at the third to fifth passages were used in the following experiments.

Immunocytochemistry analysis

Immunocytochemistry analysis was performed according to standard protocols. In brief, the third passage cells were plated in 24-well plates (Corning, USA), the media were removed after the cells reached ≥ 80% confluence and the plates were washed three times with 1×PBS. Then, the cells were fixed with 4% paraformaldehyde (Sigma-Aldrich, USA) for 15 min at room temperature. After fixation, the cells were

permeabilized with 0.5% Triton X-100 (Sigma-Aldrich, USA) for 10 min at room temperature. Next, the cells were incubated in blocking buffer (5% BSA, Thermo Fisher Scientific, USA) for 60 min. The plates were washed again and then incubated with anti-cytokeratin 1 antibody (Catalog#: ab93652, Abcam, USA) and anti-vimentin antibody (Catalog#: ab92547, Abcam, USA) overnight at 4°C. Then, the cells were incubated with secondary antibody (mouse anti-rabbit IgG; Proteintech, USA; 1:100) for 45 min at room temperature. Images were captured using an inverted microscope (Carl Zeiss, Germany). Negative controls were incubated with PBS instead of the primary antibodies.

Flow cytometric analysis of surface markers of DFSCs

The phenotype of DFSCs was determined by flow cytometric analysis. The MSC phenotyping cocktail comprised both positive (CD29-FITC, CD44/CD90-PE, BD Bioscience, USA) and negative (CD34/CD45-PE, BD Bioscience, USA) fluorochrome-conjugated monoclonal antibodies. Isotype IgG1-FITC and IgG1-PE (BD Bioscience, USA) were used as controls. The third passage DFSCs were suspended up to 1×10^7 cells/ml in 3% FBS/PBS solution, and stained with different antibodies for 30 min at 4°C, washed with PBS, resuspended in FACS buffer, and analyzed with a MOFlo™ High-performance cell sorter (Beckman Coulter, USA).

Evaluation of osteogenic and adipogenic capabilities of DFSCs

The DFSCs were loaded in 6-well plates (Corning, USA) at a cell density of 1×10^5 cells per well and cultured in α-MEM supplemented with 10% FBS. After the cells reached 80% confluence, the medium was changed to osteogenic medium (α-MEM supplemented with 10% FBS, 5 mM β-glycerophosphate, 100 nM dexamethasone, and 50 mg/ml ascorbic acid) or commercial adipogenic differentiation medium (Cyagen Biosciences, China) for the following 7 or 14 days, while α-MEM supplemented with 10% FBS was used in the control group. After 7 or 14 days of incubation, the cells were washed twice with PBS and fixed in 4% paraformaldehyde (Sigma-Aldrich, USA) for 30 min, followed by Alizarin Red staining (Cyagen Biosciences, China) to reveal calcium depositions or Oil Red O (Sigma-Aldrich, USA) for the evaluation of adipogenic differentiation. The cells were imaged with a Fluorescence Inversion Microscope System (Carl Zeiss, Germany).

Preparation of CM from DFSCs

Once the DFSCs reached 70% confluence, the cells were washed with PBS twice, and the culture medium was then changed to serum-free Ham's F-12K (Kaighn's) medium. The supernatant was collected at 24-h intervals. After centrifugation for 5 min at 1000 ×g and filtration through a 0.22 μm strainer (Millipore, USA), the collected medium was stored at -80°C immediately. It was mixed with an equal volume of serum free Ham's F-12K medium when used as DFSC-CM.

LPS-induced acute lung injury

Eight-week-old male S-D rats (n ≥ 6 per group) were anaesthetized with 10% chloral hydrate and injected through caudal vein with 2.5 mg/kg LPS[29] (*Escherichia coli*, Sigma-Aldrich, USA). Four hours post LPS-injection, rats were re-anesthetized and received a 50-μl tail intravenous instillation of DFSCs, DFSC-CM or Ham's F-12K medium. We ensured equivalence between DFSC-based and CM-based treatment by managing the same number of cells (400, 000 cells/50 μl medium) that produced 50 μl concentrated DFSC-CM. Rats were sacrificed by intraperitoneal injection of excess chloral hydrate at 24 h post-LPS for the next assessments.

Lung histological analysis

For histological examination, the lungs were fixed with 4% formaldehyde solution, embedded with paraffin, sectioned into 4-μm-thick serial sections and stained with hematoxylin and eosin (HE). Images were captured with Leica CTRMIC microscope, ten high-powered fields per lung were randomly selected and blindly scored based on a previously published protocol [39]. Accordingly, the samples were graded as follows: 0, which means normal, accounting for <15% of the space occupied by tissue and >85% occupied by alveolar space. 1+, 15%~25% occupied by tissue and 75%~85% occupied by alveolar space. 2+, 25%~50%

occupied by tissue and 50%~75% occupied by alveolar space. 3+, 50%~75% occupied by tissue and 25%~50% occupied by alveolar space; and 4+, 75%~100% occupied by tissue and 0%~25% occupied by alveolar space.

Assessment of lung permeability

Pulmonary edema due to LPS-induced increased lung permeability was measured by calculating the dry / wet weight ratios of the left upper lung lobe according to a previously described method [40]. Briefly, freshly harvested lungs were weighed (wet weights), then placed in a drying oven at 55°C for 48 hours, the dry weights were recorded, and the lung dry / wet weight ratios were calculated.

Bronchoalveolar Lavage Fluid (BALF) analysis

Lungs were perfused by injecting 2.5 ml of ice-cold PBS at 0.5-ml increments through a 20-gauge catheter inserted into the trachea. BALF was centrifuged at 400 g for 10 min and the concentrations of MCP-1, IL-1β, IL-6, TNF-α and IL-10 in the supernatants was determined by ELISA kit (Catalog#: ab179886, ab100768, ab100772, ab100785, ab100765, Abcam, UK), according to the manufacturer's instructions. The absorbance at 450 nm was measured using a microplate reader (ImmunoMini NJ1000). Triplicate reaction and three separate experiments were performed.

Lung immunofluorescence staining

The lungs were removed, embedded in OCT compound (Sakura Finetek), and cut into 10-mm-thick sections on a cryostat (Leica). The sections were then permeabilized with 0.5% Triton X-100 (Sigma-Aldrich, USA) for 20 min at room temperature, incubated in blocking buffer (5% BSA, Thermo Fisher Scientific, USA) for 60 min. The sections were washed again and then incubated with the following primary antibodies: CD11b (1:100, Catalog#: ab8879, Abcam, USA) and Arg-1 (1:50, Catalog#: 93668S, CST, USA). Anti-rabbit IgG-Alexa Fluor 594 and anti-mouse IgG-Alexa Fluor 488 was used as the secondary antibody. Images were captured using a fluorescence microscope (Carl Zeiss, Germany). The average ratio of Arg-1/CD11b double-positive cells was determined by counting ten random, non-overlapping fields at 200× magnification. At least five animals per group were used.

Real-time quantitative PCR assay

For gene expression experiments, the rat macrophage NR8383 cell line (Xiangf Bio, Shanghai, China) was loaded in 6-well plates (Corning, USA) at a cell density of 1×10^5 cells per well and cultured in Ham's F-12K medium supplemented with 20% FBS. After the cells reached 80% confluence, the medium was changed to Ham's F-12K medium or DFSC-CM, with or without LPS (0.5 mg/l, Sigma-Aldrich, USA). The cells were imaged with an inverted microscope system (Carl Zeiss, Germany). Then total RNA was isolated using TRIzol (Invitrogen, USA) at 12-h intervals, and the first-strand cDNA was synthesized using 2 μg total RNA and a TaKaRa RNA PCR kit. PCR primers are listed in Table 1. The PCR reaction conditions were 95 °C for 5 min followed by 40 cycles at 95°C for 15 s and 60°C for 30 s. Triplicate reaction and three separate experiments were performed.

Table 1. Primer sequences used in quantitative real-time polymerase chain reaction

Gene		Primers
MCP-1	Forward:	ATGCAGTTAATGCCCCACTC
	Reverse:	TTCCTTATTGGGGTCAGCAC
IL-1β	Forward:	CCCTGAACTCAACTGTGAAATAGCA
	Reverse:	CCCAAGTCAAGGGCTTGGAA
IL -6	Forward:	ATTGTATGAACAGCGATGATGCAC
	Reverse:	CCAGGTAGAAACGGAACTCCAGA
TNF-α	Forward:	TCAGTTCCATGGCCCAGAC
	Reverse:	GTTGTCTTTGAGATCCATGCCATT
IL-10	Forward:	CAGACCCACATGCTCCGAGA
	Reverse:	CAAGGCTTGGCAACCCAAGTA
Arg-1	Forward:	CTGCATATCTGCCAAGGACATC
	Reverse:	GTTCCCCAGGGTCCACATC
iNOS	Forward:	GAGGAGAGAGATCCGGTTCACA
	Reverse:	CCGCATTAGCACAGAAGCAA
β-actin	Forward:	CCTCTTTGCATGTCTCACTC
	Reverse:	AATGTCACGCACGATTTCC

ELISA

The supernatants of cultured macrophages were collected following LPS (0.5 mg/l; Sigma-Aldrich, USA) stimulation for 24 h, and the concentrations of MCP-1, IL-1β, IL-6, TNF-α and IL-10 were evaluated with commercially available ELISA kits mentioned above.

Flow cytometric analysis of macrophage polarization marker

For immunolabeling, cells were incubated with FITC-conjugated CD86 monoclonal antibody (Catalog#: 11-0860-82, ThermoFisher eBioscience, USA) and PE-conjugated CD163 monoclonal antibody (Catalog#: MA5-16657, Invitrogen, USA) at 4°C for 30 min. After incubation,

the cells were washed three times with PBS, resuspended in FACS buffer, and analyzed with a MOFlo™ High-performance cell sorter (Beckman Coulter, USA). Isotype IgG1-FITC (ThermoFisher eBioscience, USA) and IgG1-PE (BD Bioscience) were used as control.

Western blot analysis

Western blots were performed according to standard protocols. Briefly, cells were lysed with RIPA Reagent (Pierce, USA) containing 1% proteinase inhibitor (Thermo Fisher Scientific, USA) on ice for 30 min. The supernatants were harvested after centrifugation for 30 min at 12, 000 ×g. The bicinchoninic acid (BCA; Biocolors, China) method was used for estimation of total protein content. Proteins were denatured and separated by 10% SDS-polyacrylamide gels and transferred onto nitrocellulose membranes (Millipore, USA). The membranes were blocked in 5% commercial skim milk at room temperature for 1 h and probed with primary antibodies for Arg-1 (Cell Signaling Technology, USA) and iNOS (Millipore, USA) at 1:1000 or β-actin (Abcam, USA) at 1:5000 at 4°C overnight, washed, and incubated with horseradish peroxidase-conjugated secondary antibodies (Cell Signaling Technology, USA) at room temperature for 1 h. The membranes were visualized by enhanced chemiluminescence (ECL; Millipore, USA), and densitometry was performed using ImageJ software (Version 1.50i, USA).

Protein analysis of DFSC-CM

The proteins secreted by DFSCs in the CM were analyzed by a protein array according to the manufacturer's instruction (RayBiotech, USA). Briefly, protein array membranes were blocked in blocking buffer for 30 min and then incubated with DFSC-CM or serum-free Ham's F-12K medium (Sigma-Aldrich, USA) at 4°C overnight. After being washed with washing buffer, membranes were incubated with biotin-conjugated antibodies at room temperature for 2 h and then reacted with HRP-conjugated streptavidin (1:1000 dilution) at room temperature for 2 h. After incubation with detection buffer in the dark, the membranes were exposed to X-ray film, and the image was developed using a film scanner. The signal intensities were quantified by densitometry. Fold changes in protein expression were calculated.

DFSC-CM cytokine measurement and verification

The levels of TSP-1 and TGF-β3 in DFSC-CM were further confirmed by ELISA (Catalog#: CSB-E08764r and CSB-E17325r, Cusabio, China). For depletion of TSP-1 and/or TGF-β3 from DFSC-CM, anti-TSP-1 (Catalog#: NB100-2059, Novus Biologicals, USA) and/or anti-TGF-β3 (Catalog#: AF-243-NA, R&D, USA) antibodies were added to DFSC-CM. Quantitative PCR assay was performed to measure IL-6, TNF-α and IL-10 mRNA expression levels to determine the effects of the two factors on the transcription of inflammatory factors from macrophages. Western blot analysis was then performed to test the effect of the two factors on the expression levels of Arg-1 and iNOS in macrophages under inflammatory conditions.

Statistical analysis

Data are presented as the mean ± SEM of at least three independent experiments. Student's t tests were carried out for pair-wise comparisons. One-way analysis of variance with Bonferroni correction was used for multiple comparisons. Statistical significance was defined as $P < 0.05$ or 0.01 (indicated as * or **, respectively). PRISM software (Version 6.0, GraphPad Inc., La Jolla, CA) was used for data analysis.

Results

Culture and identification of macrophages and DFSCs

A rat alveolar macrophage cell line showed adherent and suspended growth with spherical cells (Fig. 1A). DFSCs were successfully isolated from rat dental follicle tissues and cultured to the third passage. DFSCs grew in an adherent manner with a typical spindle

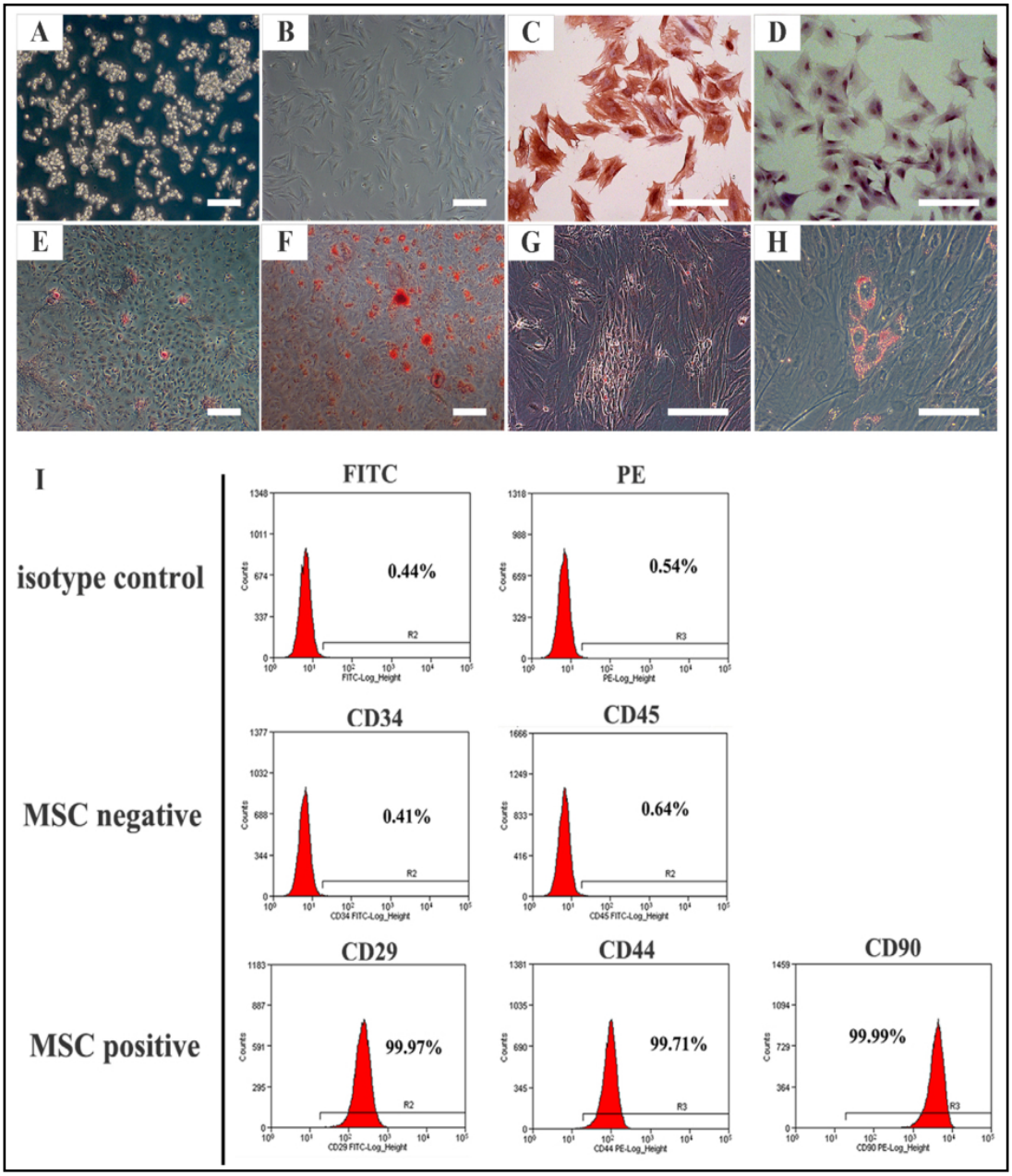

Fig. 1. Isolation and identification of DFSCs and macrophages. Representative images of macrophages (A) and DFSCs (B). Vimentin (C) and cytokeratin (D) expression in DFSCs was detected by immunohistochemistry analysis. After DFSCs were cultured under mineralizing solution for 7 days (E) and 14 days (F), mineralized nodules were detected by Alizarin Red staining. DFSCs formed lipid clusters that stained positive for Oil Red O after 7 days (G) and 14 days (H) of adipogenic induction. Scale bar: 100 μm. (I) Representative results of flow cytometric analysis showing the CD marker expression pattern in P3 DFSCs. Top panel: respective isotype controls; middle panel: MSC-negative CD markers; bottom panel: MSC-positive CD markers.

shape (Fig. 1B). Immunohistochemistry analysis showed that DFSCs were positive for the MSC marker vimentin (Fig. 1C) and negative for cytokeratin (Fig. 1D), which is a marker of epithelial cells. Flow cytometric analysis showed that the DFSCs expressed high levels of the MSC markers CD29 (99.97%), CD44 (99.71%) and CD90 (99.99%) and were negative for the hematopoietic markers CD34 (0.41%) and CD45 (0.64%) (Fig. 1I). In addition, following induction in osteogenic medium for 7 days and 14 days, DFSCs formed mineralized nodules that were visualized by Alizarin Red staining (Fig. 1E and 1F). After culture in adipogenic induction medium for 7 days and 14 days, DFSCs formed lipid droplets visualized by Oil Red O staining (Fig. 1G and 1H). These results demonstrated the multipotent differentiation ability of DFSCs.

DFSC/DFSC-CM treatment attenuated lung inflammation of LPS-induced ALI

Histological analysis revealed that LPS significantly increased the inflammatory infiltrates compared with uninjured group. This inflammatory influx was attenuated by DFSC/DFSC-CM treatment (Fig. 2A-2H). The quantitative histopathology score confirmed the phenomenon (Fig. 2J). We also found that DFSC/DFSC-CM treatment prevented the lung vascular permeability of ALI, as assessed by dry / wet ratio (Fig. 2I). The same trends were observed for the inflammatory cytokine levels in the BALF. At 24 h after LPS was administered, the levels of MCP-1, IL-1, IL-6 and TNF-α were significantly increased. When DFSC/DFSC-CM treatment was administered, the level of IL-10 increased remarkably, while the levels of MCP-1, IL-1 and TNF-α decreased, indicating attenuated inflammation (Fig. 2K-2O). Consistent with these observations, immunofluorescence analysis revealed an increased accumulation of $CD11b^{+}Arg\text{-}1^{+}$ M2 macrophages in the DFSC/DFSC-CM treatment groups (Fig. 2P and 2Q). There was no statistical difference between DFSC and DFSC-CM treatment groups, suggesting that most of the DFSC-mediated therapeutic effects were elicited through paracrine mechanisms.

DFSC-CM induced M2 macrophage polarization

In order to detect more thoroughly the occurrence of DFSC-CM-induced alternative macrophage activation *in vivo*, we employed an *in vitro* inflammation model using NR8383 macrophages. Macrophages exhibit dramatic changes in cell morphology in different polarization *in vitro*; specifically, M2-polarized cells exhibit elongated shapes compared to Ml-polarized cells [41]. We found that macrophages cultured in Ham's F-12K medium maintained a spherical cell shape, whereas macrophages cultured with DFSC-CM exhibited an elongated shape with/without LPS infection (Fig. 3A). LPS infection increased the transcription and secretion of the pro-inflammatory cytokines MCP-1, IL-1, IL-6 and TNF-α, as well as the anti-inflammatory cytokines IL-10, for 12 or 24 h, respectively. DFSC-CM treatment inhibited the production of the pro-inflammatory cytokines MCP-1, IL-1, IL-6 and TNF-α, whereas promoted the production of the anti-inflammatory cytokine IL-10 (Fig. 3B~3K). Furthermore, flow cytometric analysis showed that LPS upregulated the expression of the M1-polarizing surface marker CD86, whereas DFSC-CM treatment downregulated it (Fig. 4A). Equally, LPS downregulated the expression of the M2-polarizing surface marker CD163, whereas DFSC-CM treatment upregulated it (Fig. 4B). The macrophage polarization was further investigated using real-time PCR and western blot for the prototypical M1 and M2 markers, inducible nitric oxide synthase (iNOS) and Arg-1[42]. When cultured in DFSC-CM with LPS stimuli, macrophages exhibited significant upregulation of Arg-1 and downregulation of iNOS, whereas macrophages cultured in Ham's F-12K medium with LPS infection expressed high levels of iNOS but not Arg-1 at both the transcriptional and translational levels (Fig. 4C~4G).

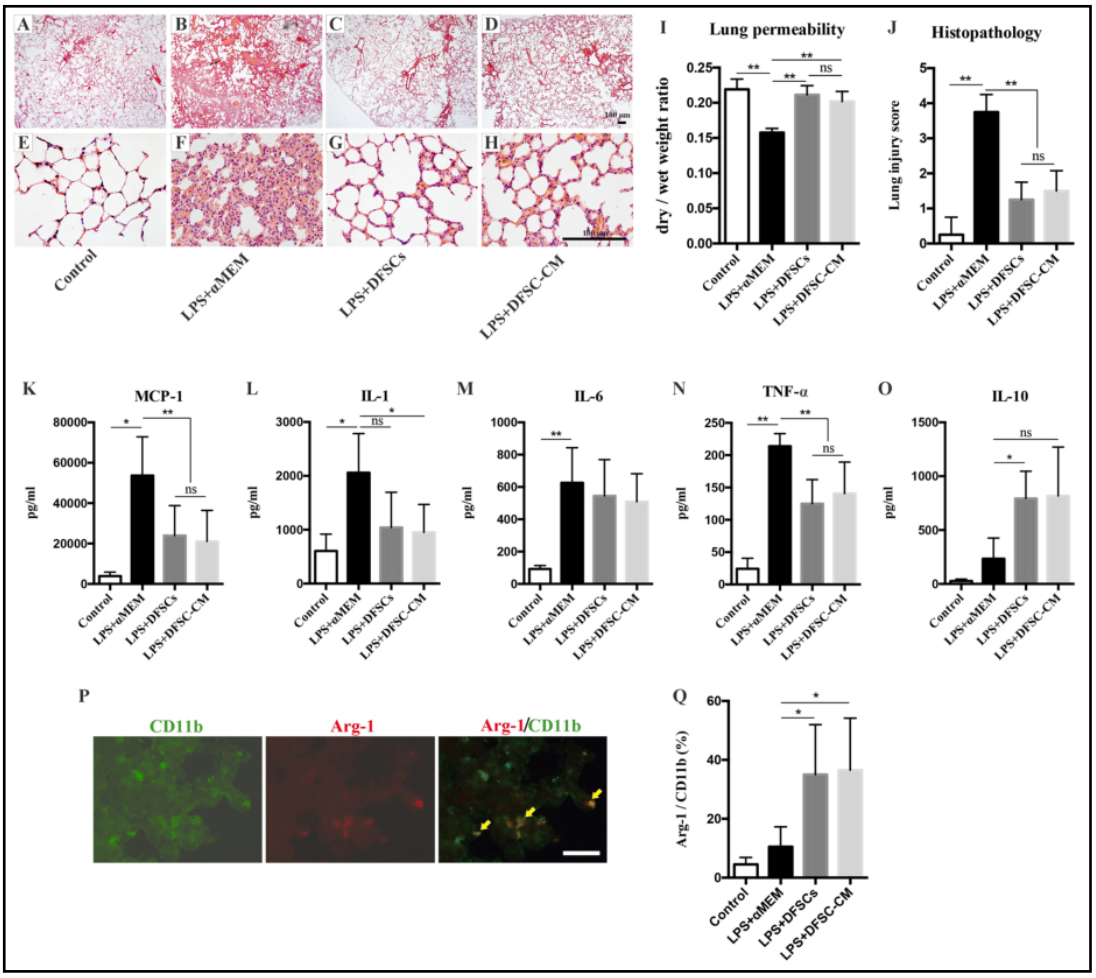

Fig. 2. DFSC/DFSC-CM treatment attenuated lung inflammation of LPS-induced ALI. (A-H) HE staining images of LPS-infected lungs after DFSC/DFSC-CM treatment. The lower panel is under higher magnification than the upper one. Scale bar: 100 μm. (I) Assessment of lung permeability by dry / wet weight ratio. (J) Quantitative histological assessment by lung injury score. The levels of the pro-inflammatory cytokines MCP-1 (K), IL-1β (L), IL-6 (M), and TNF-α (N) and the anti-inflammatory cytokine IL-10 (O) in BALF of rat ALI models treated with DFSC/DFSC-CM or Ham's F-12K medium for 24 h were assessed by ELISA. (P) Representative images of immunofluorescence staining of macrophages in lungs of rat ALI models 24 h after LPS exposure. Note that the $CD11b^+$ lung macrophages in the DFSC-CM treatment group expressed $Arg\text{-}1^+$. Scale bar: 50 μm. (Q) Quantitative assessments of the $CD11b^+Arg\text{-}1^+$ M2 macrophages in control and LPS + αMEM/DFSC/DFSC-CM treated lungs. Values are the mean ± SEM, *P<0.05, **P<0.01, ns, no significant differences.

A protein array identified potential effective factors

We performed a protein array to identify potential effective soluble factors involved in the effects of the DFSC-CM, with Ham's F-12K medium as the control. The results showed that there were 42 differentially expressed proteins between the two groups (Fig. 5A~5C), including growth factors, cytokines, chemokines, matricellular proteins, transmembrane proteins and neurotransmitters (Table 2). Among the 42 proteins, TGF-β3 and Thrombospondin-1 (TSP-1), which were significantly higher in DFSC-CM than in Ham's F-12K medium (18- and 105-fold, respectively. Fig. 5C), have previously been shown to exhibit important immunomodulatory activities [43-46].

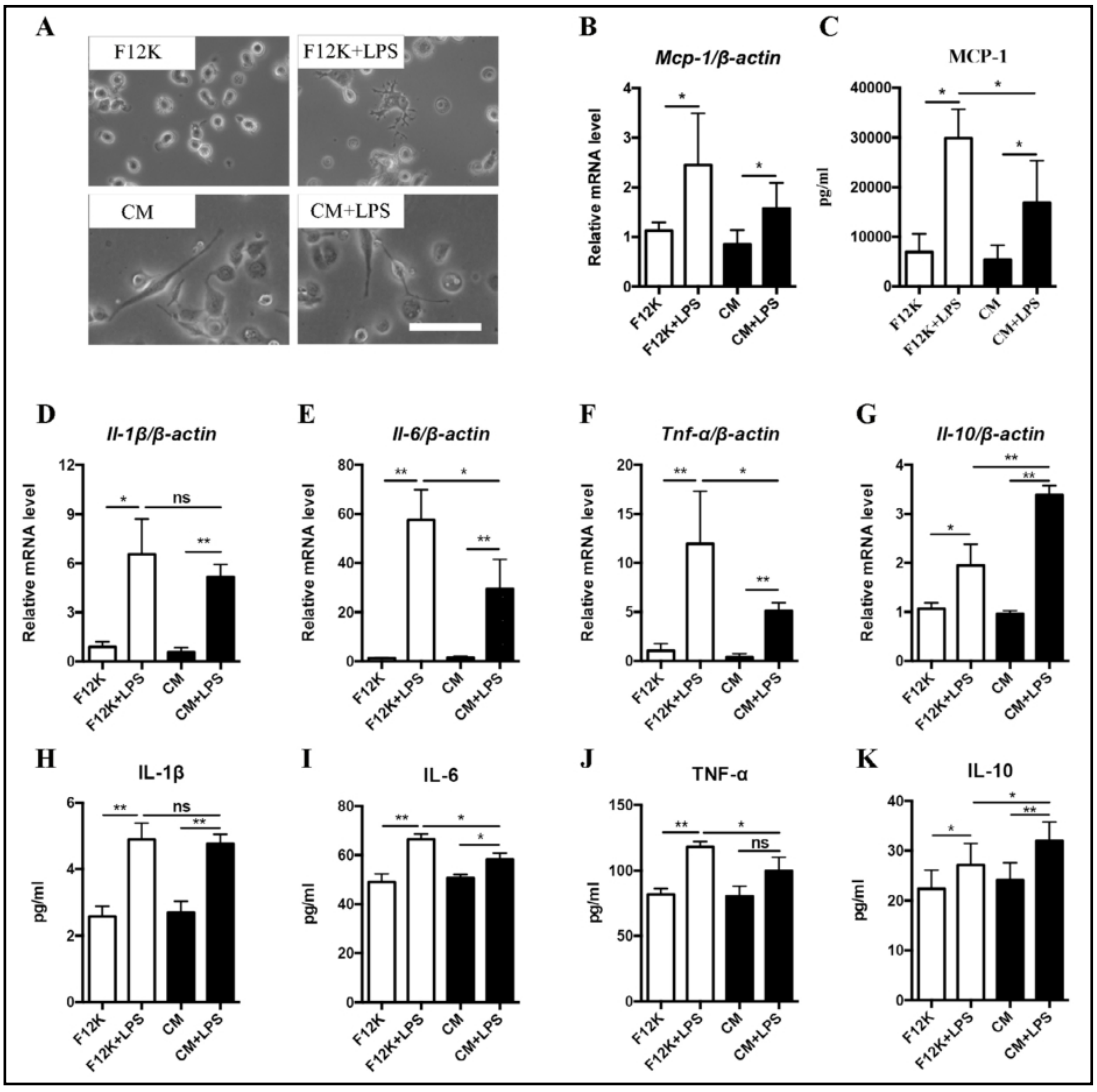

Fig. 3. DFSC-CM regulated the inflammatory condition of macrophages in vitro. (A) Images of macrophages. Macrophages cultured in F12K maintained a spherical shape, whereas those cultured in DFSC-CM exhibited an elongated phenotype with or without LPS. Scale bar: 50 μm. The mRNA levels of the pro-inflammatory cytokines MCP-1 (B), IL-1β (D), IL-6 (E), and TNF-α (F) and the anti-inflammatory cytokine IL-10 (G) in macrophages treated with DFSC-CM or Ham's F-12K medium with or without LPS for 12 h were assessed by RT-qPCR. After 24 h of co-culture of LPS-stimulated macrophages with DFSC-CM or Ham's F-12K medium, the secretions of MCP-1 (C), IL-1β (H), IL-6 (I), TNF-α (J) and IL-10 (K) in the culture media were assessed by ELISA. Values are the mean ± SEM, *P<0.05, **P<0.01, ns, no significant difference.

TSP-1 and TGF-β3 played a modulatory role in macrophage M2 polarization

We further confirmed the array results by performing ELISA on TSP-1 and TGF-β3 and explored the roles of TSP-1 and TGF-β3 in macrophage polarization. Specific neutralizing antibodies of TSP-1 and TGF-β3 were added to the DFSC-CM, and the neutralization effects were verified by ELISA (Fig. 6A and 6B). Quantitative PCR assays showed that the inhibitory effect of DFSC-CM on IL-6 transcription was attenuated by the TGF-β3 neutralizing antibody but not the TSP-1 neutralizing antibody (Fig. 6C), whereas TNF-α was unchanged when either the TSP-1 or TGF-β3 neutralizing antibody was used (Fig. 6D). Intriguingly, the DFSC-CM-mediated enhancement of IL-10 expression was partly inhibited when both TSP-1 and TGF-β3 neutralizing antibodies were used (Fig. 6E). Western blot analysis showed that DFSC-

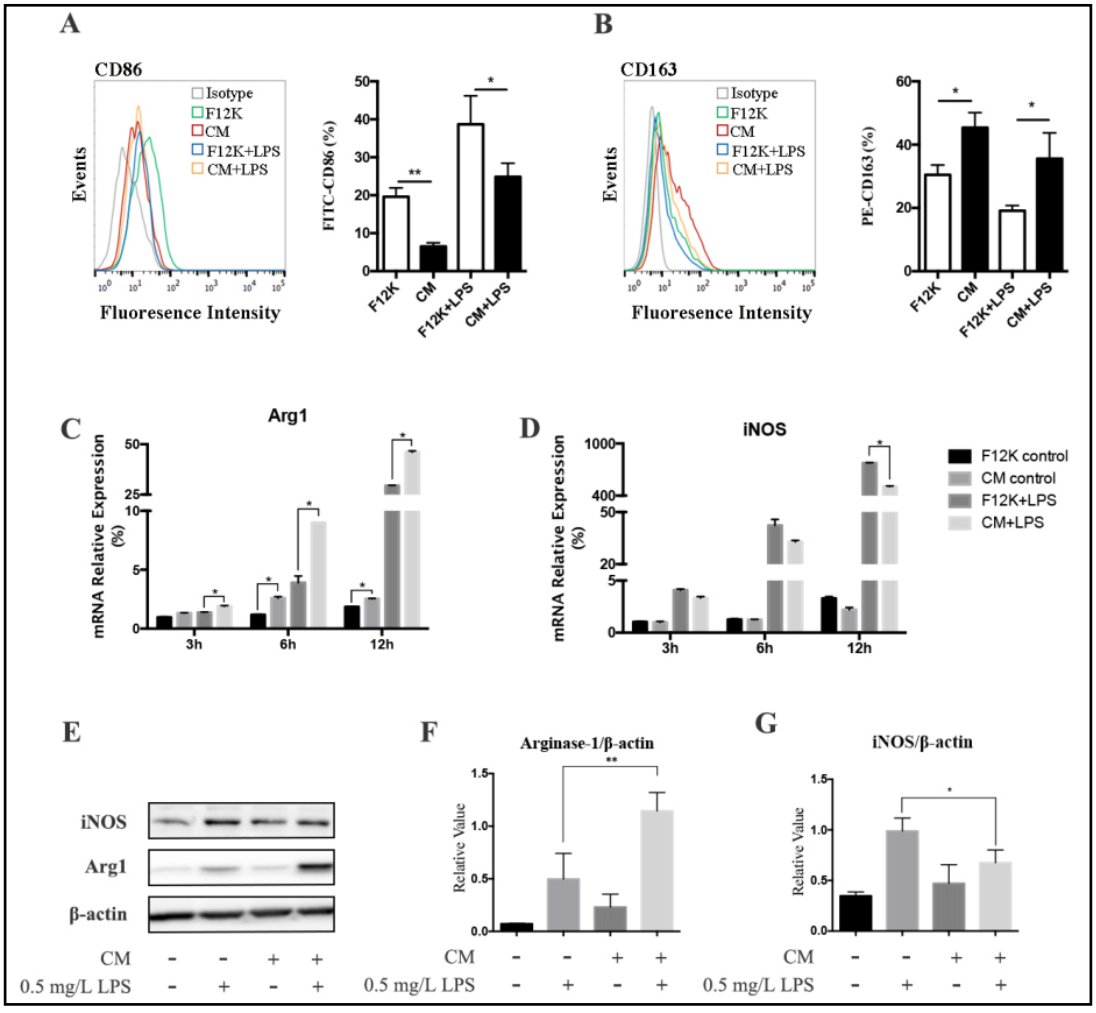

Fig. 4. DFSC-CM induced macrophage polarization to a M2 phenotype. (A, B) Flow cytometric analysis for the M1-polarizing surface marker CD86 and M2-polarizing surface marker CD163 on macrophages treated with DFSC-CM or Ham's F-12K medium with or without LPS for 6 h. Values are the mean ± SEM, *P<0.05, **P<0.01. (C, D) RT-qPCR for Arg-1 and iNOS in macrophages treated with DFSC-CM or Ham's F-12K medium with or without LPS for 3 h, 6 h and 12 h. Values are the mean ± SEM, *P<0.05. (E~G) Western blot analysis of Arg-1, iNOS and β-actin in macrophages treated with DFSC-CM or Ham's F-12K medium with or without LPS for 12 h. Values are the mean ± SEM, *P<0.05, **P<0.01.

Table 2. Differentially expressed (>2 folds) soluble factors in DFSC-CM compared with Ham's F-12K Medium

Categories	Factors	Count
Growth factors	TGF-β3, BDNF, VEGF, VEGF-C, basic-FGF, FGF-BP	6
Cytokines	IL-1β, IL-2, TNF-α, GM-CSF	4
Chemokines	MCP-1, MDC, MIP-2, MIP-3α, LIX, CX3CL1	6
Matricellular protein	TSP-1, TIMP-1, TIMP-2, MMP-2, OPN, FSL1	6
Transmembrane protein	CCR4, CXCR4, CD80, IL-1 R6, Nrp-2, NGFR, EGFR, TIE-2, GFR α-1, GFR α-2	10
Intracellular protein	β-Catenin, Ubiquitin	2
Enzymes	IDE, AMPK α1, MuSK, CSK	4
Neurotransmitter	Orexin A	1
TNF alpha ligand	TRAIL	1
Hormone	ACTH, Leptin	2
Total		42

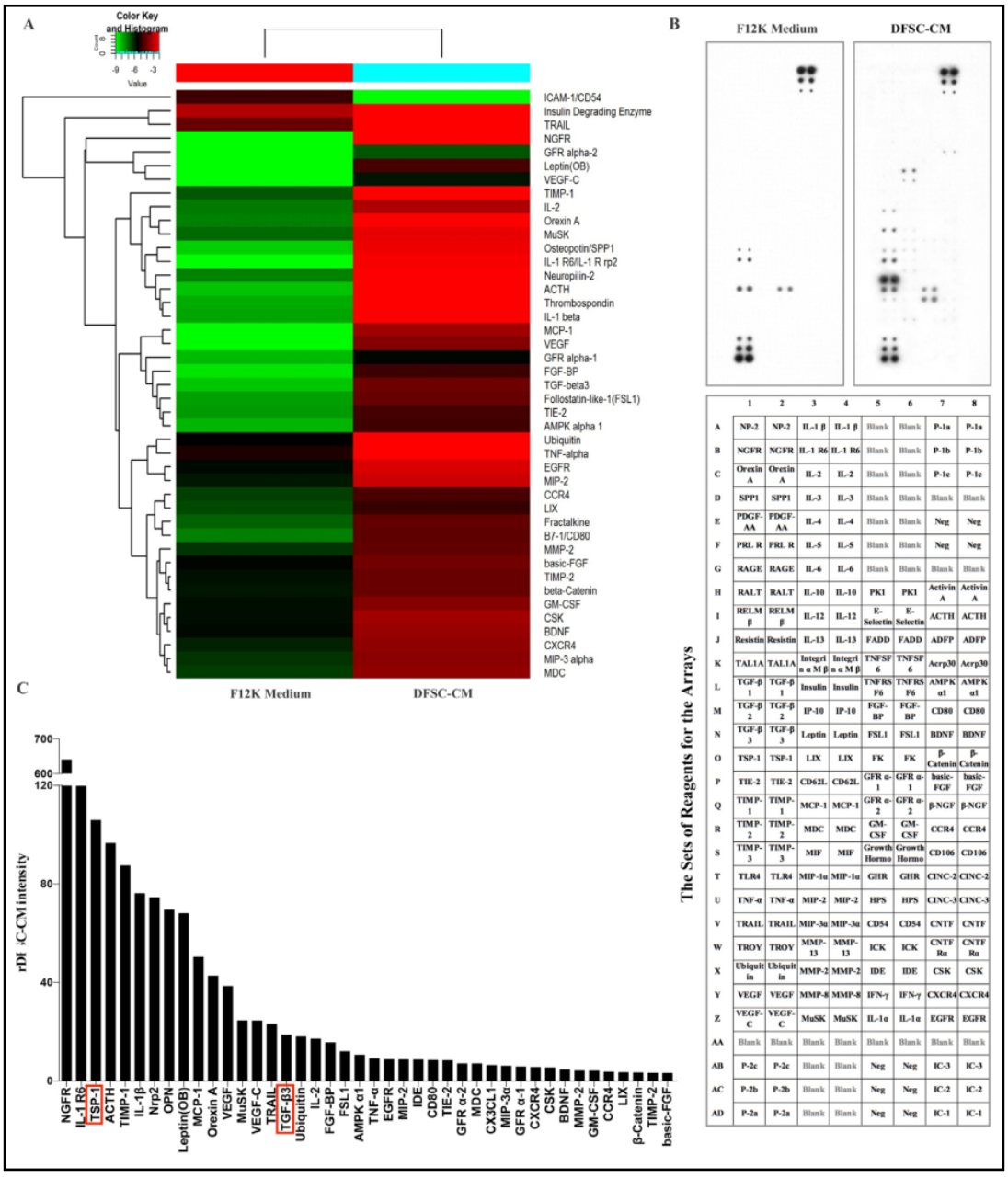

	1	2	3	4	5	6	7	8
A	NP-2	NP-2	IL-1 β	IL-1 β	Blank	Blank	P-1a	P-1a
B	NGFR	NGFR	IL-1 R6	IL-1 R6	Blank	Blank	P-1b	P-1b
C	Orexin A	Orexin A	IL-2	IL-2	Blank	Blank	P-1c	P-1c
D	SPP1	SPP1	IL-3	IL-3	Blank	Blank	Blank	Blank
E	PDGF-AA	PDGF-AA	IL-4	IL-4	Blank	Blank	Neg	Neg
F	PRL R	PRL R	IL-5	IL-5	Blank	Blank	Neg	Neg
G	RAGE	RAGE	IL-6	IL-6	Blank	Blank	Blank	Blank
H	RALT	RALT	IL-10	IL-10	PKI	PKI	Activin A	Activin A
I	RELM β	RELM β	IL-12	IL-12	E-Selectin	E-Selectin	ACTH	ACTH
J	Resistin	Resistin	IL-13	IL-13	FADD	FADD	ADFP	ADFP
K	TAL1A	TAL1A	Integrin α M β	Integrin α M β	TNFSF6	TNFSF6	Acrp30	Acrp30
L	TGF-β1	TGF-β1	Insulin	Insulin	TNFRSF6	TNFRSF6	AMPK α1	AMPK α1
M	TGF-β2	TGF-β2	IP-10	IP-10	FGF-BP	FGF-BP	CD80	CD80
N	TGF-β3	TGF-β3	Leptin	Leptin	FSL1	FSL1	BDNF	BDNF
O	TSP-1	TSP-1	LIX	LIX	FK	FK	β-Catenin	β-Catenin
P	TIE-2	TIE-2	CD62L	CD62L	GFR α-1	GFR α-1	basic-FGF	basic-FGF
Q	TIMP-1	TIMP-1	MCP-1	MCP-1	GFR α-2	GFR α-2	β-NGF	β-NGF
R	TIMP-2	TIMP-2	MDC	MDC	GM-CSF	GM-CSF	CCR4	CCR4
S	TIMP-3	TIMP-3	MIF	MIF	Growth Hormo	Growth Hormo	CD106	CD106
T	TLR4	TLR4	MIP-1α	MIP-1α	GHR	GHR	CINC-2	CINC-2
U	TNF-α	TNF-α	MIP-2	MIP-2	HPS	HPS	CINC-3	CINC-3
V	TRAIL	TRAIL	MIP-3α	MIP-3α	CD54	CD54	CNTF	CNTF
W	TROY	TROY	MMP-13	MMP-13	ICK	ICK	CNTF Rα	CNTF Rα
X	Ubiquitin	Ubiquitin	MMP-2	MMP-2	IDE	IDE	CSK	CSK
Y	VEGF	VEGF	MMP-8	MMP-8	IFN-γ	IFN-γ	CXCR4	CXCR4
Z	VEGF-C	VEGF-C	MuSK	MuSK	IL-1α	IL-1α	EGFR	EGFR
AA	Blank	Blank	Blank	Blank	Blank	Blank	Blank	Blank
AB	P-2c	P-2c	Blank	Blank	Neg	Neg	IC-3	IC-3
AC	P-2b	P-2b	Blank	Blank	Neg	Neg	IC-2	IC-2
AD	P-2a	P-2a	Blank	Blank	Neg	Neg	IC-1	IC-1

Fig. 5. Protein analysis of the DFSC-CM by RayBiotech Protein Array. (A) Clustering analysis of differentially expressed proteins between DFSC-CM and Ham's F-12K medium. (B) After incubation with HRP-conjugated streptavidin, the signals were visualized by chemiluminescence. (C) The protein array revealed 42 differentially expressed (>2-fold) proteins in DFSC-CM compared with Ham's F-12K medium, among which TSP-1 and TGF-β3 were upregulated by 105-fold and 18-fold, respectively.

CM increased Arg-1 levels in macrophages. However, this effect was attenuated by addition of either TSP-1 or TGF-β3 neutralizing antibodies and significantly suppressed when both antibodies were added (Fig. 6F). Although neutralizing antibodies had no obvious effects on iNOS expression (Fig. 6G), our results provided conclusive evidence that TSP-1 and TGF-β3 were positively associated with macrophage M2 polarization.

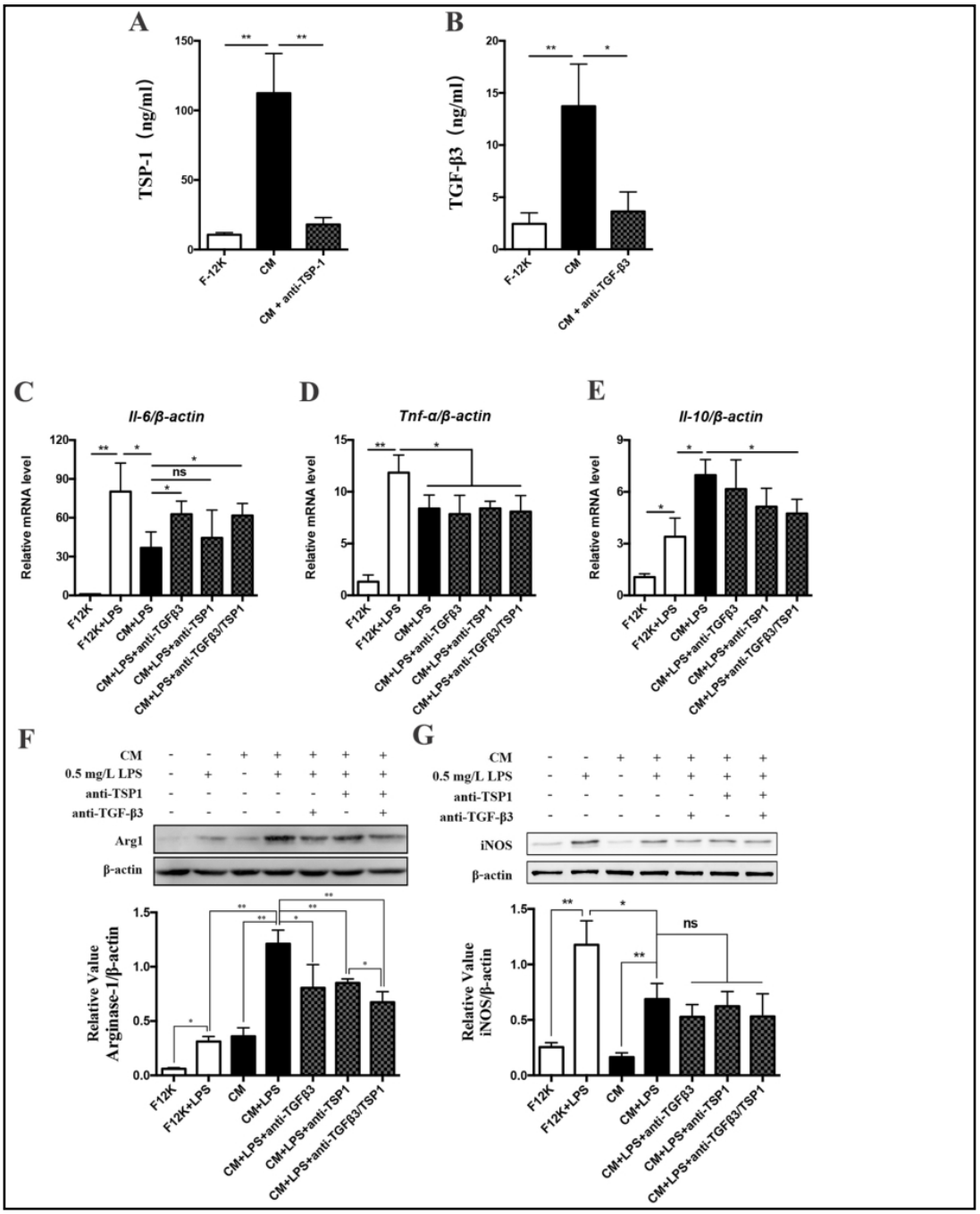

Fig. 6. The verification of the potential effective factors in DFSC-CM. Quantification of TSP-1 (A) and TGF-β3 (B) by ELISA tested in DFSC-CM and Ham's F-12K medium before and after adding specific neutralizing antibodies. Values are the mean ± SEM, *P<0.05, **P<0.01. RT-qPCR for IL-6 (C), TNF-α (D) and IL-10 (E) in macrophages treated with DFSC-CM with neutralizing antibodies against TSP-1 and/or TGF-β3 after LPS stimulation. Values are the mean ± SEM, *P<0.05, **P<0.01, ns, no significant differences. Representative Western blot from macrophages treated with DFSC-CM with neutralizing antibodies against TSP-1 and/or TGF-β3 after LPS stimulation shows the protein levels of Arg-1 (F) and iNOS (G) at 12 h. Values are the mean ± SEM, *P<0.05, **P<0.01, ns, no significant differences.

Discussion

In the present study, we provide evidence that the therapeutic benefits of DFSCs are due to paracrine mechanisms. The intravenous administration of DFSC-CM reduced the lung edema and inflammatory injury *in vivo*, this effect was comparable with the administration of an equivalent number of DFSCs. And DFSC-CM induced an anti-inflammatory M2 translation of macrophages exposed to LPS *in vitro* and *in vivo*. We also identified a previously unrecognized set of M2-like macrophage inducers, TGF-β3 and TSP-1, by secretome analysis of the DFSC-CM.

In the development of ALI, neutrophils and macrophages are activated to eliminate pathogens, however, it brings tissue damage by releasing antimicrobial compounds at the same time [31]. Monocyte chemoattractant protein-1 (MCP-1), also known as CCL2, is closely related to the recruitment of macrophages to the lungs [47] and prolonged elevation of inflammatory cytokines in ALI[48]. In the present study, MCP-1 was suppressed *in vitro* in macrophages and in rat models of ALI after DFSC-CM treatment, which would contribute to the reduction of the infiltration of inflammatory cells *in vivo*. Our results are in good agreement with previous studies demonstrating that MCP-1 is essential for inflammatory infiltration in ALI [47, 48] and other reports showing that MSC treatment remarkably decreased the injury score and neutrophil infiltration in the lung [30, 49]. Our data demonstrated the anti-inflammatory effects of DFSCs and DFSC-CM, at least to some extent, based on their ability to inhibit inflammatory infiltration.

The present study suggests that DFSCs and DFSC-CM promote anti-inflammatory macrophages M2 translation. Ionescu *et al.* have reported that the activation of M2 macrophages is one of the mechanisms by which MSCs alleviate lung injury [32]. In consistent with their reports, we found that alveolar macrophages from lungs treated with DFSCs and DFSC-CM had elevated expression of M2 macrophage-specific marker Arg-1 compared with that of untreated LPS rats. Our further study also showed that in the *in vitro* inflammation model using NR8383 macrophages, DFSC-CM treatment reduced the release of the pro-inflammatory cytokines IL-1β, IL-6 and TNF-α and increased the release of the anti-inflammatory cytokine IL-10 under LPS stimulation. In addition, when LPS-treated macrophages were exposed to DFSC-CM, the expression levels of M2 macrophage-specific markers CD163 and Arg-1 increased, whereas the expression of M1 macrophage-specific markers CD86 and iNOS decreased. To the best of our knowledge, we demonstrated here for the first time that DFSCs promoted the macrophage polarization towards the M2 phenotype through paracrine effects.

Indeed, the paracrine mode of MSCs opens up new therapeutic perspectives. Various soluble factors secreted by MSCs, including IL-4[50], IL-13[51], prostaglandin E2 (PGE2) [52], and tumor necrosis factor-α-induced gene/protein 6 (TSG-6)[53], have been shown to play a critical role in modulating inflammatory processes and macrophage polarization towards the M2 phenotype in animal models of sepsis [54], acute kidney injury [17], experimental colitis [18], spinal cord injury [19], and skin wounds [1]. To determine the key factors responsible for macrophage polarization towards the M2 phenotype induced by DFSC-CM, we performed a protein array, which revealed that rDFSCs could release many secreted proteins, including immunomodulatory factors, growth factors, cytokines, chemokines and neurotrophic factors, thus providing useful information for future studies. In a similar manner, Schinköthe et al [55]. analyzed the secreting profile of human MSCs to attain the first large range of factors they secrete and categorized these into functional groups: immunosuppressive, angiogenic, anti-apoptotic, and pro-proliferative factors. Intriguingly, among factors that may account for the macrophage polarity conversion, we found that DFSC-CM did not contain classical M2-inducers. Based on bioinformatics analysis, TGF-β3 and TSP-1 were implied to be candidate molecules for further studies.

Studies have shown both pro- and anti-inflammatory functions of TGF-β3[56, 57], indicating its distinctive contributions to immunological activities. TGF-β3 could promote scar-free repair in wound healing, which highlighted its anti-inflammatory effect and therapeutic potential [58-60]. Our present study showed that DFSC-CM was rich in TGF-β3 and inhibited IL-6 production of LPS-treated macrophages via it *in vitro*, which was consistent with a previous study showing that TGF-β3 significantly suppressed both IL-6 transcripts and secretion in human cleft lip and palate fibroblasts [61]. Intriguingly, IL-6 levels were not significantly reduced post-DFSC/DFSC-CM treatment *in vivo*, which was

contrary to a recent finding that MSCs treatment decreased IL-6 levels in the BALF after *S. pneumoniae* induced ALI[62]. We speculate that this might be on account of that the effect of MSCs on IL-6 production varies depending on the bacterial species [63]. Another possible reason is that *in vitro* conditions only reflected the macrophage responses, and other cells like neutrophils [64] can also contribute to IL-6 production *in vivo*, leading to differences between *in vitro* and *in vivo* results. Furthermore, our findings that the incubation of DFSC-CM with a neutralizing anti-TGF-β3 antibody reduced the expression of the M2 polarization marker Arg-1 indicated that TGF-β3 might play a role in DFSC-CM-directed macrophage M2 polarization, even though the expression of the M1 polarization marker iNOS was not affected. Further studies are needed to reveal the underlying mechanisms. To the best of our knowledge, the present study was the first to uncover the potential roles of DFSC-secreted TGF-β3 in macrophage polarization switch.

TSP-1, a member of the matricellular TSP protein family, is secreted by a variety of normal and transformed cells [65]. A significant high level of TSP-1 was observed in DFSC-CM. Targeting TSP-1 with a specific neutralizing antibody had a measurable impact on Arg-1 expression of macrophages, which was consistent with previous studies by Chen and colleagues showing that the absence of TSP-1 led to an increase in the ratio of Arg-1^{-}CD68^{+} M1 macrophages in a mouse autoimmune uveoretinitis model [44]. These results suggested that TSP-1 could promote the expression of Arg-1, but the specific mechanism has not yet been revealed. In addition, previous studies showed that by disrupting the interaction between CD47 and CD14 on human macrophages, TSP-1 limited the activation of NF-κB/AP-1 by LPS, resulting in inhibition of inflammatory cytokine production [43]. In the present study, however, addition of neutralizing antibodies against TSP-1 to DFSC-CM had little effect on the expression levels of IL-6, TNF-α and iNOS of macrophages, which may be due to the different regulatory effects of TSP-1 in different environments [43, 66, 67]. Intriguingly, we found that IL-10 expression was not significantly reduced by the addition of either TGF-β3 or TSP-1 neutralizing antibodies, but IL-10 was significantly inhibited when both neutralizing antibodies were added to DFSC-CM. These findings indicated that TGF-β3 and TSP-1 might have a synergistic effect on IL-10 expression of macrophages. Yehualaeshet *et al.* demonstrated that TSP-1 could interact with and convert latent TGF-β1 into active TGF-β1[68], indicating a crosstalk between TSP-1 and TGF-β1. Since TGF-β3 and TGF-β1 share a similar structure, ligand binding site and biological features [69], there might also be an interaction between TGF-β3 and TSP-1 that synergistically promoted IL-10 expression.

Notably, DFSC-CM also contained significantly increased levels of potential protective factors, suggesting that other mechanisms might explain the therapeutic benefits of DFSC-CM in this model. TIMP-1 was increased 87-fold in DFSC-CM compared with control medium. TIMP-1 is the major endogenous regulator of matrix metalloproteinase with an important role in improving wound healing through its pro-proliferation and anti-apoptosis effects [70]. Another molecule, TRAIL, was increased 23-fold in DFSC-CM compared with control medium. TRAIL mediates the anti-inflammatory benefits by inhibiting the proliferation and activation of T cells in the peripheral immune system [71, 72]. We also found that AMPK-α1 was increased 10-fold in DFSC-CM compared with control medium. AMPK-α1 is crucial in regulating metabolism [73]. Recent study shows that metformin alleviates capillary injury during LPS-induced ALI via AMPK-α1[74]. A 3-fold increase of FGF-2 was observed in DFSC-CM compared with control group. Mice treated with FGF-2-loaded heparin-conjugated fibrin showed significantly reduced inflammation and enhanced neovascularization [75].Therefore, TIMP-1, TRAIL, AMPK-α1, FGF-2 and many others might also be of vital importance in anti-inflammatory effects in DFSC-CM although it still needs further study.

Conclusion

Taken together, our data provides direct *in vivo* and *in vitro* evidence that DFSCs exert their therapeutic benefits through a paracrine way. We have identified a novel set of M2 inducers, TSP-1 and TGF-β3, from DFSC-CM. These findings support the hypothesis that DFSCs, a unique population of dental-derived MSCs with accessible tissue source, ease of isolation and rapid proliferation, are a promising cell source for MSC-based immunotherapy.

Acknowledgements

This study was supported by National Natural Science Foundation of China (81670983), Guangdong Provincial Science and Technology Plan Program (2015A020212004), and Guangdong Provincial Natural Science Foundation (2017A030308011).

Disclosure Statement

The authors declare that they have no competing interests.

References

1 Huang SCC, Everts B, Ivanova Y, O'Sullivan D, Nascimento M, Smith AM, Beatty W, Love-Gregory L, Lam WY, O'Neil CM, Yan C, Du H, Abumrad NA, Urban JF, Artyomov MN, Pearce EL, Pearce EJ: Cell-intrinsic lysosomal lipolysis is essential for alternative activation of macrophages. Nature Immunology 2014;15:846-855.
2 Gentek R, Molawi K, Sieweke MH: Tissue macrophage identity and self-renewal. Immunol Rev 2014;262:56-73.
3 Varol C, Mildner A, Jung S: Macrophages: development and tissue specialization. Annu Rev Immunol 2015;33:643-675.
4 Ginhoux F, Jung S: Monocytes and macrophages: developmental pathways and tissue homeostasis. Nat Rev Immunol 2014;14:392-404.
5 Satoh T, Nakagawa K, Sugihara F, Kuwahara R, Ashihara M, Yamane F, Minowa Y, Fukushima K, Ebina I, Yoshioka Y, Kumanogoh A, Akira S: Identification of an atypical monocyte and committed progenitor involved in fibrosis. Nature 2017;541:96-101.
6 Yang YF, Zhou YD, Hu JC, Luo FL, Xie Y, Shen YY, Bian WX, Yin ZN, Li HL, Zhang XL: Ficolin-A/2, acting as a new regulator of macrophage polarization, mediates the inflammatory response in experimental mouse colitis. Immunology 2017;151:433-450.
7 Ivashkiv LB: Epigenetic regulation of macrophage polarization and function. Trends Immunol 2013;34:216-223.
8 Barron L, Wynn TA: Fibrosis is regulated by Th2 and Th17 responses and by dynamic interactions between fibroblasts and macrophages. Am J Physiol Gastrointest Liver Physiol 2011;300:G723-728.
9 Murray PJ, Wynn TA: Protective and pathogenic functions of macrophage subsets. Nat Rev Immunol 2011;11:723-737.
10 Brancato SK, Albina JE: Wound macrophages as key regulators of repair: origin, phenotype, and function. Am J Pathol 2011;178:19-25.
11 Pittenger MF, Mackay AM, Beck SC, Jaiswal RK, Douglas R, Mosca JD, Moorman MA, Simonetti DW, Craig S, Marshak DR: Multilineage potential of adult human mesenchymal stem cells. Science (New York, NY) 1999;284:143-147.
12 Uccelli A, Moretta L, Pistoia V: Mesenchymal stem cells in health and disease. Nat Rev Immunol 2008;8:726-736.
13 Zhang QZ, Su WR, Shi SH, Wilder-Smith P, Xiang AP, Wong A, Nguyen AL, Kwon CW, Le AD: Human gingiva-derived mesenchymal stem cells elicit polarization of m2 macrophages and enhance cutaneous wound healing. Stem Cells 2010;28:1856-1868.
14 Gao F, Chiu SM, Motan DA, Zhang Z, Chen L, Ji HL, Tse HF, Fu QL, Lian Q: Mesenchymal stem cells and immunomodulation: current status and future prospects. Cell Death Dis 2016;7:e2062.
15 Blazquez R, Sanchez-Margallo FM, Alvarez V, Uson A, Casado JG: Surgical meshes coated with mesenchymal stem cells provide an anti-inflammatory environment by a M2 macrophage polarization. Acta Biomater 2016;31:221-230.
16 Park HJ, Oh SH, Kim HN, Jung YJ, Lee PH: Mesenchymal stem cells enhance alpha-synuclein clearance via M2 microglia polarization in experimental and human parkinsonian disorder. Acta Neuropathol 2016;132:685-701.

17 Zullo J, Nadel E, Rabadi M, Baskind M, Rajdev M, Demaree C, Vasko R, Chugh S, Lamba R, Goligorsky M, Ratliff B: The Secretome of Hydrogel-Coembedded Endothelial Progenitor Cells and Mesenchymal Stem Cells Instructs Macrophage Polarization in Endotoxemia. Stem Cells Transl Med 2015;4:852-861.
18 Simovic Markovic B, Nikolic A, Gazdic M, Nurkovic J, Djordjevic I, Arsenijevic N, Stojkovic M, Lukic M, Volarevic V: Pharmacological Inhibition of Gal-3 in Mesenchymal Stem Cells Enhances Their Capacity to Promote Alternative Activation of Macrophages in Dextran Sulphate Sodium-Induced Colitis. Stem Cells Int 2016;2016:2640746.
19 Nakajima H, Uchida K, Guerrero A, Watanabe S, Sugita D, Takeura N, Yoshida A, Long G, Wright K, Johnson W, Baba H: Transplantation of mesenchymal stem cells promotes an alternative pathway of macrophage activation and functional recovery after spinal cord injury. J Neurotrauma 2012;29:1614-1625.
20 Li Z, Jiang CM, An S, Cheng Q, Huang YF, Wang YT, Gou YC, Xiao L, Yu WJ, Wang J: Immunomodulatory properties of dental tissue-derived mesenchymal stem cells. Oral Dis 2014;20:25-34.
21 Tormin A, Li O, Brune JC, Walsh S, Schutz B, Ehinger M, Ditzel N, Kassem M, Scheding S: CD146 expression on primary nonhematopoietic bone marrow stem cells is correlated with in situ localization. Blood 2011;117:5067-5077.
22 Mao JJ, Prockop DJ: Stem cells in the face: tooth regeneration and beyond. Cell Stem Cell 2012;11:291-301.
23 Yang B, Qiu Y, Zhou N, Ouyang H, Ding J, Cheng B, Sun J: Application of Stem Cells in Oral Disease Therapy: Progresses and Perspectives. Front Physiol 2017;8:197.
24 Shimojima C, Takeuchi H, Jin S, Parajuli B, Hattori H, Suzumura A, Hibi H, Ueda M, Yamamoto A: Conditioned Medium from the Stem Cells of Human Exfoliated Deciduous Teeth Ameliorates Experimental Autoimmune Encephalomyelitis. J Immunol 2016;196:4164-4171.
25 Ishikawa J, Takahashi N, Matsumoto T, Yoshioka Y, Yamamoto N, Nishikawa M, Hibi H, Ishigro N, Ueda M, Furukawa K, Yamamoto A: Factors secreted from dental pulp stem cells show multifaceted benefits for treating experimental rheumatoid arthritis. Bone 2016;83:210-219.
26 Yamaza T, Kentaro A, Chen C, Liu Y, Shi Y, Gronthos S, Wang S, Shi S: Immunomodulatory properties of stem cells from human exfoliated deciduous teeth. Stem Cell Res Ther 2010;1:5.
27 Makino Y, Yamaza H, Akiyama K, Ma L, Hoshino Y, Nonaka K, Terada Y, Kukita T, Shi S, Yamaza T: Immune therapeutic potential of stem cells from human supernumerary teeth. J Dent Res 2013;92:609-615.
28 Yildirim S, Zibandeh N, Genc D, Ozcan EM, Goker K, Akkoc T: The Comparison of the Immunologic Properties of Stem Cells Isolated from Human Exfoliated Deciduous Teeth, Dental Pulp, and Dental Follicles. Stem Cells Int 2016;2016:4682875.
29 Ionescu L, Byrne RN, van Haaften T, Vadivel A, Alphonse RS, Rey-Parra GJ, Weissmann G, Hall A, Eaton F, Thébaud B: Stem cell conditioned medium improves acute lung injury in mice: *in vivo* evidence for stem cell paracrine action. American Journal of Physiology-Lung Cellular and Molecular Physiology 2012;303:L967-L977.
30 Xiang B, Chen L, Wang X, Zhao Y, Wang Y, Xiang C: Transplantation of Menstrual Blood-Derived Mesenchymal Stem Cells Promotes the Repair of LPS-Induced Acute Lung Injury. Int J Mol Sci 2017;18:689.
31 van Haaften T, Byrne R, Bonnet S, Rochefort GY, Akabutu J, Bouchentouf M, Rey-Parra GJ, Galipeau J, Haromy A, Eaton F, Chen M, Hashimoto K, Abley D, Korbutt G, Archer SL, Thebaud B: Airway delivery of mesenchymal stem cells prevents arrested alveolar growth in neonatal lung injury in rats. Am J Respir Crit Care Med 2009;180:1131-1142.
32 Ionescu L, Byrne RN, van Haaften T, Vadivel A, Alphonse RS, Rey-Parra GJ, Weissmann G, Hall A, Eaton F, Thebaud B: Stem cell conditioned medium improves acute lung injury in mice: *in vivo* evidence for stem cell paracrine action. Am J Physiol Lung Cell Mol Physiol 2012;303:L967-977.
33 Peng Z, Liu L, Wei X, Ling J: Expression of Oct-4, SOX-2, and MYC in dental papilla cells and dental follicle cells during in-vivo tooth development and in-vitro co-culture. European journal of oral sciences 2014;122:251-258.
34 Zhang X, Du Y, Ling J, Li W, Liao Y, Wei X: Dickkopf-related protein 3 negatively regulates the osteogenic differentiation of rat dental follicle cells. Mol Med Rep 2017;15:1673-1681.
35 Chen C, Xie N, Ling J, Du Y, Gu H: Proteomic analysis of the effects of CSF-1 and IL-1alpha on dental follicle cells. Mol Med Rep 2016;14:2405-2414.
36 Du Y, Ling J, Wei X, Ning Y, Xie N, Gu H, Yang F: Wnt/beta-catenin signaling participates in cementoblast/osteoblast differentiation of dental follicle cells. Connect Tissue Res 2012;53:390-397.

37 Du Y, Gu HJ, Gong QM, Yang F, Ling JQ: HSP25 affects the proliferation and differentiation of rat dental follicle cells. Int J Oral Sci 2009;1:72-80.
38 Zhan Z, Xie X, Cao H, Zhou X, Zhang XD, Fan H, Liu Z: Autophagy facilitates TLR4- and TLR3-triggered migration and invasion of lung cancer cells through the promotion of TRAF6 ubiquitination. Autophagy 2014;10:257-268.
39 Hofbauer B, Saluja AK, Bhatia M, Frossard J-L, Lee H-S, Bhagat L, Steer ML: Effect of recombinant platelet-activating factor acetylhydrolase on two models of experimental acute pancreatitis. Gastroenterology 1998;115:1238-1247.
40 Gupta N, Su X, Popov B, Lee JW, Serikov V, Matthay MA: Intrapulmonary delivery of bone marrow-derived mesenchymal stem cells improves survival and attenuates endotoxin-induced acute lung injury in mice. J Immunol 2007;179:1855-1863.
41 McWhorter FY, Wang T, Nguyen P, Chung T, Liu WF: Modulation of macrophage phenotype by cell shape. Proc Natl Acad Sci U S A 2013;110:17253-17258.
42 Labonte AC, Sung SJ, Jennelle LT, Dandekar AP, Hahn YS: Expression of scavenger receptor-AI promotes alternative activation of murine macrophages to limit hepatic inflammation and fibrosis. Hepatology 2017;65:32-43.
43 Stein EV, Miller TW, Ivins-O'Keefe K, Kaur S, Roberts DD: Secreted Thrombospondin-1 Regulates Macrophage Interleukin-1beta Production and Activation through CD47. Sci Rep 2016;6:19684.
44 Chen M, Copland DA, Zhao J, Liu J, Forrester JV, Dick AD, Xu H: Persistent inflammation subverts thrombospondin-1-induced regulation of retinal angiogenesis and is driven by CCR2 ligation. Am J Pathol 2012;180:235-245.
45 Rubtsov YP, Rudensky AY: TGFbeta signalling in control of T-cell-mediated self-reactivity. Nat Rev Immunol 2007;7:443-453.
46 Tsunawaki S, Sporn M, Ding A, Nathan C: Deactivation of macrophages by transforming growth factor-beta. Nature 1988;334:260-262.
47 Wu Z, Wang Z, Xu P, Zhang M, Cheng L, Gong B: A Novel Finding: Macrophages Involved in Inflammation Participate in Acute Aortic Dissection Complicated with Acute Lung Injury. Curr Mol Med 2017;17:568-579.
48 Coates BM, Staricha KL, Koch CM, Cheng Y, Shumaker DK, Budinger GRS, Perlman H, Misharin AV, Ridge KM: Inflammatory Monocytes Drive Influenza A Virus-Mediated Lung Injury in Juvenile Mice. J Immunol 2018;200:2391-2404.
49 Taki T, Masumoto H, Funamoto M, Minakata K, Yamazaki K, Ikeda T, Sakata R: Fetal mesenchymal stem cells ameliorate acute lung injury in a rat cardiopulmonary bypass model. J Thorac Cardiovasc Surg 2017;153:726-734.
50 Park H, Oh S, Kim H, Jung Y, Lee P: Mesenchymal stem cells enhance α-synuclein clearance via M2 microglia polarization in experimental and human parkinsonian disorder. Acta Neuropathol 2016;132:685-701.
51 Ali I, Aertgeerts S, Le Blon D, Bertoglio D, Hoornaert C, Ponsaerts P, Dedeurwaerdere S: Intracerebral delivery of the M2 polarizing cytokine interleukin 13 using mesenchymal stem cell implants in a model of temporal lobe epilepsy in mice. Epilepsia 2017;58:1063-1072.
52 Chiossone L, Conte R, Spaggiari G, Serra M, Romei C, Bellora F, Becchetti F, Andaloro A, Moretta L, Bottino C: Mesenchymal Stromal Cells Induce Peculiar Alternatively Activated Macrophages Capable of Dampening Both Innate and Adaptive Immune Responses. Stem Cells 2016;34:1909-1921.
53 Qi Y, Jiang D, Sindrilaru A, Stegemann A, Schatz S, Treiber N, Rojewski M, Schrezenmeier H, Vander Beken S, Wlaschek M, Böhm M, Seitz A, Scholz N, Dürselen L, Brinckmann J, Ignatius A, Scharffetter-Kochanek K: TSG-6 released from intradermally injected mesenchymal stem cells accelerates wound healing and reduces tissue fibrosis in murine full-thickness skin wounds. J Invest Dermatol 2014;134:526-537.
54 Zullo JA, Nadel EP, Rabadi MM, Baskind MJ, Rajdev MA, Demaree CM, Vasko R, Chugh SS, Lamba R, Goligorsky MS, Ratliff BB: The Secretome of Hydrogel-Coembedded Endothelial Progenitor Cells and Mesenchymal Stem Cells Instructs Macrophage Polarization in Endotoxemia. Stem Cells Transl Med 2015;4:852-861.
55 Schinkothe T, Bloch W, Schmidt A: *In vitro* secreting profile of human mesenchymal stem cells. Stem Cells Dev 2008;17:199-206.
56 Lee Y, Awasthi A, Yosef N, Quintana FJ, Xiao S, Peters A, Wu C, Kleinewietfeld M, Kunder S, Hafler DA, Sobel RA, Regev A, Kuchroo VK: Induction and molecular signature of pathogenic TH17 cells. Nat Immunol 2012;13:991-999.

57 Okamura T, Sumitomo S, Morita K, Iwasaki Y, Inoue M, Nakachi S, Komai T, Shoda H, Miyazaki J, Fujio K, Yamamoto K: TGF-beta3-expressing CD4+CD25(-)LAG3+ regulatory T cells control humoral immune responses. Nat Commun 2015;6:6329.
58 Ferguson MW, O'Kane S: Scar-free healing: from embryonic mechanisms to adult therapeutic intervention. Philos Trans R Soc Lond B Biol Sci 2004;359:839-850.
59 Martin P, D'Souza D, Martin J, Grose R, Cooper L, Maki R, McKercher SR: Wound Healing in the PU.1 Null Mouse—Tissue Repair Is Not Dependent on Inflammatory Cells. Curr Biol 2003;13:1122-1128.
60 Wulff BC, Parent AE, Meleski MA, DiPietro LA, Schrementi ME, Wilgus TA: Mast Cells Contribute to Scar Formation during Fetal Wound Healing. J Invest Dermatol 2012;132:458-465.
61 Baroni T, Carinci P, Bellucci C, Lilli C, Becchetti E, Carinci F, Stabellini G, Pezzetti F, Caramelli E, Tognon M, Bodo M: Cross-talk between interleukin-6 and transforming growth factor-beta3 regulates extracellular matrix production by human fibroblasts from subjects with non-syndromic cleft lip and palate. J Periodontol 2003;74:1447-1453.
62 Asami T, Ishii M, Namkoong H, Yagi K, Tasaka S, Asakura T, Suzuki S, Kamo T, Okamori S, Kamata H, Zhang H, Hegab AE, Hasegawa N, Betsuyaku T: Anti-inflammatory roles of mesenchymal stromal cells during acute Streptococcus pneumoniae pulmonary infection in mice. Cytotherapy 2018;20:302-313.
63 Fung TC, Bessman NJ, Hepworth MR, Kumar N, Shibata N, Kobuley D, Wang K, Ziegler CGK, Goc J, Shima T, Umesaki Y, Sartor RB, Sullivan KV, Lawley TD, Kunisawa J, Kiyono H, Sonnenberg GF: Lymphoid-Tissue-Resident Commensal Bacteria Promote Members of the IL-10 Cytokine Family to Establish Mutualism. Immunity 2016;44:634-646.
64 Rigonato-Oliveira NC, MacKenzie B, Bachi ALL, Oliveira MC, Santos-Dias A, Brandao-Rangel MAR, Delle H, Costa-Guimaraes T, Damaceno-Rodrigues NR, Dulley LH, Benetti MA, Malfitano C, de Angelis K, Albertini R, Oliveira APL, Abbasi A, Northoff H, Vieira RP: Aerobic exercise inhibits acute lung injury: from mouse to human evidence Exercise reduced lung injury markers in mouse and in cells. Exerc Immunol Rev 2018;24:48-56.
65 Lopez-Dee Z, Pidcock K, Gutierrez LS: Thrombospondin-1: multiple paths to inflammation. Mediators Inflamm 2011;2011:296069.
66 Xing T, Wang Y, Ding WJ, Li YL, Hu XD, Wang C, Ding A, Shen JL: Thrombospondin-1 Production Regulates the Inflammatory Cytokine Secretion in THP-1 Cells Through NF-kappaB Signaling Pathway. Inflammation 2017;40:1606-1621.
67 Kirsch T, Woywodt A, Klose J, Wyss K, Beese M, Erdbruegger U, Grossheim M, Haller H, Haubitz M: Endothelial-derived thrombospondin-1 promotes macrophage recruitment and apoptotic cell clearance. J Cell Mol Med 2010;14:1922-1934.
68 Yehualaeshet T, O'Connor R, Green-Johnson J, Mai S, Silverstein R, Murphy-Ullrich JE, Khalil N: Activation of Rat Alveolar Macrophage-Derived Latent Transforming Growth Factor β-1 by Plasmin Requires Interaction with Thrombospondin-1 and its Cell Surface Receptor, CD36. Am J Pathol 1999;155:841-851.
69 Okamura T, Morita K, Iwasaki Y, Inoue M, Komai T, Fujio K, Yamamoto K: Role of TGF-beta3 in the regulation of immune responses. Clin Exp Rheumatol 2015;33:S63-69.
70 Lao G, Ren M, Wang X, Zhang J, Huang Y, Liu D, Luo H, Yang C, Yan L: Human tissue inhibitor of metalloproteinases-1 improved wound healing in diabetes through its anti-apoptotic effect. Experimental dermatology 2017;DOI: 10.1111/exd.13442
71 Lunemann JD, Waiczies S, Ehrlich S, Wendling U, Seeger B, Kamradt T, Zipp F: Death ligand TRAIL induces no apoptosis but inhibits activation of human (auto)antigen-specific T cells. J Immunol 2002;168:4881-4888.
72 Wandinger KP, Lunemann JD, Wengert O, Bellmann-Strobl J, Aktas O, Weber A, Grundstrom E, Ehrlich S, Wernecke KD, Volk HD, Zipp F: TNF-related apoptosis inducing ligand (TRAIL) as a potential response marker for interferon-beta treatment in multiple sclerosis. Lancet 2003;361:2036-2043.
73 Hardie DG, Ross FA, Hawley SA: AMP-Activated Protein Kinase: A Target for Drugs both Ancient and Modern. Chem Biol 2012;19:1222-1236.
74 Zhang X, Shang F, Hui L, Zang K, Sun G: The alleviative effects of metformin for lipopolysaccharide-induced acute lung injury rat model and its underlying mechanism. Saudi Pharm J 2017;25:666-670.
75 Yang HS, Bhang SH, Hwang JW, Kim DI, Kim BS: Delivery of Basic Fibroblast Growth Factor Using Heparin-Conjugated Fibrin for Therapeutic Angiogenesis. Tissue Eng Pt A 2010;16:2113-2119.